



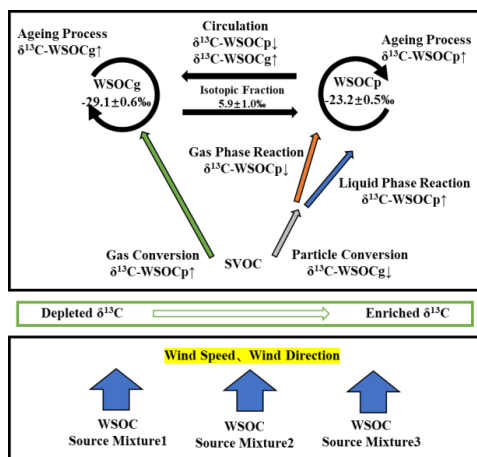
1 High-resolution observation of stable carbon isotope ratios of water-soluble organic
2 carbon in particle/gas phases at an urban site in China: Using an improved isotope
3 ratio mass spectrometry method

4 Hao-Ran Yu, Yan-Lin Zhang*, Fang Cao, Xiao-Ying Yang, Tian Xie, Yu-Xian Zhang, Yongwen
5 Xue

6 ¹ School of Applied Meteorology, Nanjing University of Information Science & Technology,
7 Nanjing 210044, China.

8 ² Atmospheric Environment Center, Joint Laboratory for International Cooperation on Climate and
9 Environmental Change, Ministry of Education (ILCEC), Nanjing University of Information
10 Science & Technology, Nanjing 210044, China.

11 **TOC:**



12

13 **Key points:**

- 14 1. Obvious fractionation exists between $\delta^{13}\text{C-WSOCp}$ and $\delta^{13}\text{C-WSOCg}$, and there is obvious
15 diurnal variation of it.
- 16 2. Mutual conversion between WSOCp and WSOCg only happens during daytime, but radiation
17 intensity has no effect on the formation mechanism and gas-particle distribution mechanism of
18 WSOC.
- 19 3. Gas-particle distribution mechanism of WSOC was restricted by meteorological conditions,
20 precursor gaseous pollutants, gaseous oxidants and acid gases, and is accompanied by the
21 formation of secondary inorganic ion component



23 **Abstract:** A high time resolution synchronous sampling method along with determination of stable
24 carbon isotopes of gaseous water-soluble organic carbon (WSOC_g) and particulate water-soluble
25 organic carbon (WSOC_p) was realized in this research through equipment modification and method
26 improvement. It was found that WSOC_g has significant higher concentration than WSOC_p and a
27 more depleted $\delta^{13}\text{C}$. Both concentrations of WSOC_p and WSOC_g have the seasonal variation
28 characteristics of high in winter (WSOC_p= $15.7\pm 3.9\mu\text{g}/\text{m}^3$; WSOC_g= $42.4\pm 6.0\mu\text{g}/\text{m}^3$) and low in
29 summer (WSOC_p= $5.9\pm 1.8\mu\text{g}/\text{m}^3$; WSOC_g= $25.2\pm 5.2\mu\text{g}/\text{m}^3$), with greater increase in WSOC_p
30 (167%) than that in WSOC_g (68%). During wintertime, WSOC_p and WSOC_g had similar daily
31 variation characteristics of concentration, and opposite daily variation characteristics of $\delta^{13}\text{C}$.
32 WSOC_p had a bimodal distribution with obvious low value at sunrise and sunset, while $\delta^{13}\text{C}$ -
33 WSOC_p had a unimodal distribution with low in daytime ($-24.6\pm 1.1\%$) and high in nighttime ($-$
34 $22.3\pm 1.7\%$). WSOC_g and $\delta^{13}\text{C}$ -WSOC_g had same distribution with high in daytime and
35 ($49.3\pm 8.8\mu\text{g}/\text{m}^3$; $-27.9\pm 1.1\%$) low in nighttime ($38.3\pm 4.6\mu\text{g}/\text{m}^3$; $-29.9\pm 0.4\%$). Combining the $\delta^{13}\text{C}$
36 variation characteristics with the synchronous observation results of meteorological conditions,
37 gaseous precursor pollutants, gaseous oxidants, gaseous acids and fine particle components, the
38 restriction factors of WSOC gas-particle distribution mechanism were discussed. The presence of
39 radiation rather than its intensity decided whether generations process of WSOC_p and WSOC_g are
40 divided, for $\delta^{13}\text{C}$ -WSOC of two phases showed significant correlation only during daytime.
41 Meteorological conditions, gaseous precursor pollutants, gaseous oxidants and gaseous acids restrict
42 the gas particle distribution of WSOC by affecting the aging process of WSOC_p and WSOC_g, gas-
43 particle conversion ratio of semi-volatile organic compounds (SVOC) and the gas phase and liquid
44 phase generation ratio of WSOC_p. At the same time, the gas-particle distribution process of WSOC
45 is strongly related to the formation of secondary inorganic ions (nitrate, sulfate, ammonium), and
46 the gas-particle distribution between gaseous nitrous acid and nitrite.

47 **Keywords:** gas phase, particle phase, WSOC, $\delta^{13}\text{C}$.

48 1. Introduction

49 Carbonaceous aerosols were considered to be one of the largest sources of uncertainty in the
50 estimation of global radiative forcing in climate change research (Bond, et al., 2013; Pöschl, 2005),
51 and water soluble organic carbon is an important component of carbonaceous aerosols, which has
52 an important impact on haze formation, human health and the earth's radiation balance. Generally,



53 carbonaceous aerosols include organic carbon (OC), elemental carbon (EC) and carbonate carbon
54 (CC) aerosols. For the content of CC is generally low (<5%) and its properties are relatively stable,
55 research of atmospheric environment and climate mainly focuses on EC and OC, which can account
56 for 20-50% of the mass concentration of PM_{2.5}(Pöschl, 2005). According to the water solubility of
57 OC, it can be divided into water insoluble organic carbon (WIOC) and water-soluble organic carbon
58 (WSOC). Most of WSOC comes from biomass burning or secondary organic aerosol (SOA)(Kondo,
59 et al., 2007; Weber, et al., 2007), mainly contains dicarboxylic acids, ketoacids, dicarbonyl
60 compounds, long-chain fatty acids and short-chain monocarboxylic acids, which can contribute 20-
61 80% of OC mass concentration. However, there exist quite different distribution characteristics of
62 WSOC in different regions(Fu, et al., 2013; Ho, et al., 2006; Miyazaki, et al., 2006; Wang, et al.,
63 2012).

64 The formation of WSOC is closely related to gas-particle distribution, emission source and
65 meteorological conditions. The synchronous study on particle phase of WSOC (WSOCp) and gas
66 phase of WSOC (WSOCg) is helpful to understand the sources and atmospheric process of SOA.
67 Though WSOCp was considered to characterize SOA to some extent when the direct contribution
68 of biomass combustion can be neglected(Kondo, et al., 2007; Weber, et al., 2007), more and more
69 evidences showed an important contribution of WSOCg to the generation of SOA. Similar to
70 WSOCp, WSOCg can be generated from secondary conversion of VOCs, in addition to the direct
71 emission such as biomass burning and fossil fuel combustion(Carlton, et al., 2009; Liu, et al., 2012;
72 Liu, et al., 2012; Meng, et al., 2014). There is evidence that VOCs emitted from natural or man-
73 made sources can be oxidized to WSOCg in the atmosphere (Carlton and Turpin, 2013; Sareen, et
74 al., 2017), and liquid phase reaction of WSOCg absorbed by cloud water or aerosol liquid water is
75 one of the important ways to formation of SOA(Liu, et al., 2012). In addition, a large part of the
76 intermediate products of isoprene oxidation, which was considered to be the most important
77 precursor of SOA, can constitute WSOCg, including glyoxal, methylglyoxal, and isoprene
78 epoxydiol, and some low molecular organic acids (such as formic acid and acetic acid) (Carlton, et
79 al., 2009; El-Sayed, et al., 2015). However, there is still great uncertainty in assessing the
80 contribution of natural and man-made sources to WSOCg under the background of compound
81 atmospheric pollution. Only qualitative or semi quantitative calculation can be carried out by means
82 of characteristic molecular markers, while the results based on model simulation are limited by the



83 understanding of atmospheric mechanism and lack of direct observation evidence for verification.

84 Previous researches had studied on gas-particle distribution mechanism of WSOC by
85 synchronously measuring the concentration of WSOCp and WSOCg. The research in Atlanta
86 reported that the WSOCg in summer ranged from 1.1 to 73.1 $\mu\text{gC m}^{-3}$, average 13.7 $\mu\text{gC m}^{-3}$, which
87 was obviously higher than WSOCp ($3.3 \pm 1.8 \mu\text{gC m}^{-3}$), but had a certain linear correlation with
88 WSOCp (Hennigan, et al., 2009). Later, research in Atlanta and Los Angeles found that WSOCp
89 and WSOCg had similar diurnal variation rules, and both reached the highest value after noon (about
90 14:00), indicating important contribution of secondary reaction (Zhang, et al., 2012). It was also
91 found that difference of precursors may lead to the change of WSOC in the gas-particle distribution
92 relationship. The variation of WSOCp in Atlanta was controlled by the aerosol liquid water content
93 (ALWC) under the influence of humidity, which was similar to WSOCp in Chongming island,
94 China (Lv, et al., 2022). While variation of WSOCp in Los Angeles was independent of ALWC, but
95 depended on OC concentration (Zhang, et al., 2012). Similarly, variation of WSOCp in Prague was
96 found to depend on TC in gas phase. There may be obvious regional differences in the gas-particle
97 distribution relationship of WSOC.

98 Stable carbon isotope ratio ($^{13}\text{C}/^{12}\text{C}$, $\delta^{13}\text{C}$) can provide important information about the sources
99 and atmospheric chemical conversion processes of carbonaceous aerosols. $\delta^{13}\text{C}$ was generally used
100 to distinguish sources of carbonaceous aerosols, such as C3 and C4 plant, vehicle exhaust, coal
101 combustion and other fossil sources (Cao, et al., 2011). However, $\delta^{13}\text{C}$ has a mass dependent isotope
102 fractionation phenomenon, leading an isotope variation apart from effects of sources. The secondary
103 reaction of VOCs to generate SOA is an important source of WSOCp (Kondo, et al., 2007; Weber,
104 et al., 2007), and aerosols formed by VOCs usually have a more depleted $\delta^{13}\text{C}$ than the
105 precursor (Anderson, et al., 2004; Rudolph, et al., 2003; Rudolph, et al., 2000). For example, isotope
106 fractionation in the process of biosynthesis of isoprene will lead to $\delta^{13}\text{C}$ of isoprene $2.6 \pm 0.9 \%$
107 smaller than it in blade (Rudolph, et al., 2003). The main scavenging pathway of VOCs is its reaction
108 with OH radical and ozone, and these atmospheric oxidants tend to react with VOCs depleted $\delta^{13}\text{C}$
109 (reverse dynamic isotope effect), resulting in the $\delta^{13}\text{C}$ enrichment of residual VOCs in the
110 atmosphere and $\delta^{13}\text{C}$ dilution of particles as oxidation products (Anderson, et al., 2004; Rudolph, et
111 al., 2003; Rudolph, et al., 2000). Some studies have also shown that $\delta^{13}\text{C}$ will be enriched in particles
112 during ageing process, such as process in which binary acid reacts with OH and is removed in the



113 form of CO₂/CO (Aggarwal and Kawamura, 2008; Noziere, et al., 2015; Pavuluri, et al., 2011; Wang,
114 et al., 2012; Zhang, et al., 2016). Measurement based on high time resolution observation of δ¹³C-
115 WSOCp and δ¹³C-WSOCg will provide a new perspective for deep understanding of the whole life
116 cycle of WSOC.

117

118 2. Data and methods

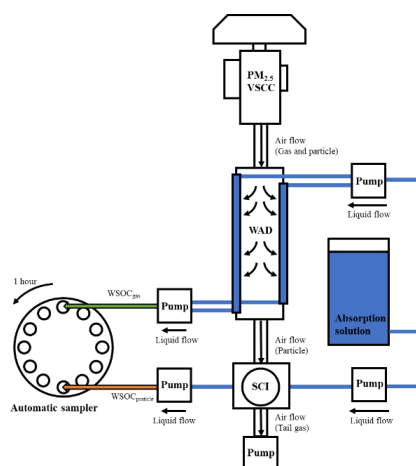
119 2.1 Sampling and chemical analysis

120 The two phases WSOC samples were collected from 4 to 14 December of 2021 in Nanjing, a
121 megacity in eastern China. The sampling site is located at the agrometeorological station of
122 Nanjing University of Information Science and Technology, which is close to a busy traffic road
123 and surrounded by a large number of industrial factories. The WSOC mass concentration was
124 measured with the total organic carbon analyzer (TOC-L, Shimadzu, Japan), analyzed along with
125 peak area signal of isotope ratio mass spectrometer (MAT253, Thermo Fisher Scientific, USA).
126 Six anions (F⁻, Cl⁻, NO₂⁻, NO₃⁻, SO₄²⁻ and PO₄³⁻), five cations (Na⁺, NH₄⁺, K⁺, Mg²⁺, and Ca²⁺)
127 and three organic acids (formic, acetic, and oxalic acids) were measured using the ion
128 chromatography system (IC-5000, Thermo Fisher Scientific, USA). The PM_{2.5} and pollution gas
129 concentration were observed at Pukou environmental supervising station, and the meteorological
130 data was observed at Pukou meteorological station. The radiation data are from the shared data of
131 the comprehensive meteorological observation base of Nanjing University of Information Science
132 and Technology. During 3 June and 13 July of 2021, 202 samples were collected with ions and
133 WSOC concentration analyzed, which was used as summer data compared with winter mass
134 concentration.

135 A wet annular denuder (WAD) combined with scrub and impactor aerosol collector (SCI)
136 (IGAC, Machinshop, Taiwan, China) was used for water-soluble organic carbon collecting. Based
137 on the principle of gas diffusion, gas phase of WSOC was absorbed and washed away by the
138 absorption liquid flowing through the pipe wall of WAD. The steam generated by the SCI will
139 capture the particle phase of WSOC by collision and condensation after that, and the sample will be
140 collected by inertial impact in liquid form. A very sharp cut cyclone (VSCC) was set in the entrance
141 of to filter particles above 2.5 μm. WSOCp and WSOCg samples were collected in glass tubes by an
142 automatic rotating device at the end of system. The system can collect 20 mL WSOCp and 20 mL



143 WSOC_g samples from 1 m³ of air every hour. The system pipeline should be flushed with ultrapure
144 water for one week before each sampling to reduce blank pollution, and the glass tubes were
145 prebaked at 450°C for 6 h before use. Blank pollution of WSOC accounted 8% of average WSOC_p
146 and 3% of average WSOC_g. To analyze filter-based WSOC_p, PM_{2.5} aerosol samples were also
147 collected onto quartz fiber filters which were prebaked at 450 °C for 6 h using an automatic sampler
148 (DHA-80, Digital, Switzerland). Sampling flow rate was 500L/min and the time resolution was 1 h.
149 Daily average of filter-based WSOC_p accounted for 81% of WSOC_p determined by IGAC system.
150 It was similar to a percentage of 89% in a study using IGAC system at Chongming island(Anderson,
151 et al., 2008). It may accounted to the speciation of the sampled organic gases which resulted in the
152 variation in denuder efficiency(Anderson, et al., 2008). However, the lower WSOC_p sampling
153 efficiency of denuder compared with filter is still hard to explain, for evaporation loss of OC,
154 especially volatile and semi volatile carbonaceous components, was proved to happen on filter
155 surfaces(Lewtas, et al., 2001; Yang, et al., 2021). It is considered that the denuder had passive
156 sampling capability of WSOC, but it's hard to estimate the artifacts accurately for there was a
157 variation of passive sampling along with pollution level(Jingyue, et al., 2010).



158
159 Fig 1. High resolution WSOC_p and WSOC_g synchronous sampling device

160
161 2.2 Stable carbon isotope analysis

162 $\delta^{13}\text{C}$ -WSOC values were analyzed with a GasbenchII-IRMS system. Due to the low content of
163 WSOC in liquid samples, an improved method was used for determination of $\delta^{13}\text{C}$ in this study,



164 mainly included pretreatment improvement and instrument transformation. Subsequent data
165 analysis used person correlation analysis.

166 2.2.1 Sample pretreatment and isotope determination

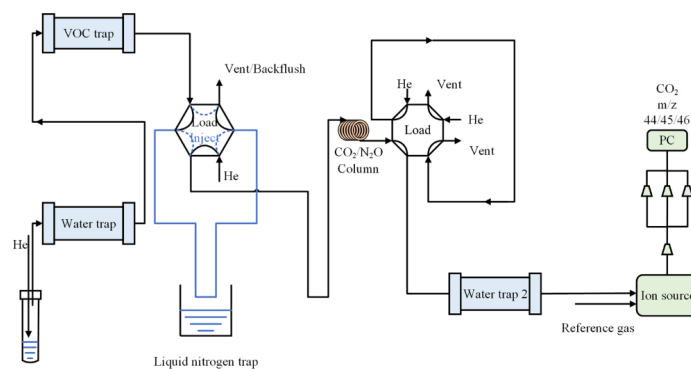
167 The wet oxidation method was used to pretreat the samples in order to convert WSOC to CO₂.
168 It took 4mL filtered liquid sample (0.22µm, Hydrophobic PTFE needle filter), along with 1mL
169 acidifier (100µL 85% phosphoric acid, soluble in 100mL Milli-Q water), standing for 1h in order to
170 remove WSIC (HCO₃⁻, CO₃²⁻). Otherwise, WSIC may cause a isotope fractionation of about
171 0.2 ‰(Suto and Kawashima, 2018). Oxidizer was prepared by 1g potassium persulfate (K₂S₂O₈,
172 99.99%), 50µL of phosphoric acid (H₃PO₄, 85%) and 100mL of Milli-Q water. It took 0.5mL of
173 oxidizer injected into a 12mL pre-purged sealed headspace bottle (100mL/min high purity helium
174 purging for 1 min). 2mL liquid sample was then injected into headspace bottle, and heated in sand
175 bath with 100°C for 1h. It took 6h to wait for complete condensation of water vapor after sand bath
176 to avoid leakage of headspace bottle or damage of IRMS.

177 CO₂ blank in headspace bottle mainly came from three parts, OC of oxidizer/acidifier(Fisseha,
178 et al., 2006), CO₂ dissolved in Milli-Q water and residual air CO₂ during purging. During the CO₂
179 blank test, the signal response of the mass spectrometer to samples was controlled to be 80 area/µgC.
180 Compared with helium purging under liquid level after sample injection, a method of helium purging
181 before sample injection could effectively eliminate the impact of residual CO₂ in the air (<2area).
182 In addition, CO₂ blank signal would increase around 10area (about 0.1µgC) with each 50mg increase
183 of K₂S₂O₈. And CO₂ blank signal would increase around 20area (about 0.25µgC) with each 1mL
184 increase of liquid in headspace bottle. In contrast, CO₂ blank is more affected by liquid content. And
185 this part of CO₂ blank couldn't be controlled by He purging or pre-heating. By controlling the
186 sample volume, reducing the oxidant concentration and injection volume, the total CO₂ blank signal
187 finally reached around 30area (about 0.3µgC), approximately 19% of the average carbon content of
188 WSOC sample.

189 The Gasbench-IRMS system and determination method were improved in this method. The
190 system used high-purity helium as carrier gas. Sample gas was pushed through the water trap
191 (magnesium perchlorate) and VOC trap in the preconcentration unit (Precon) by helium at a pressure
192 of 1.7bar. After 260s of freeze enrichment and impurity removal in liquid nitrogen trap, helium at a
193 pressure of 0.6bar was switched by rotating of six-way valve in Precon, pushing sample gas into gas



194 chromatographic column (Polra PLOT Q) to separate N_2O and CO_2 . Back purge valve of front
195 pipeline was open at the same time to purge the sample injection pipeline. Finally, sample gas
196 entered IRMS for $\delta^{13}C$ determination after water removal through a Nafion permeation tube. It took
197 a total of 24min in this method, and the determination accuracy can reach 0.25 ‰ above $1\mu gC$, can
198 reach 0.53 ‰ above $0.5\mu gC$.



199

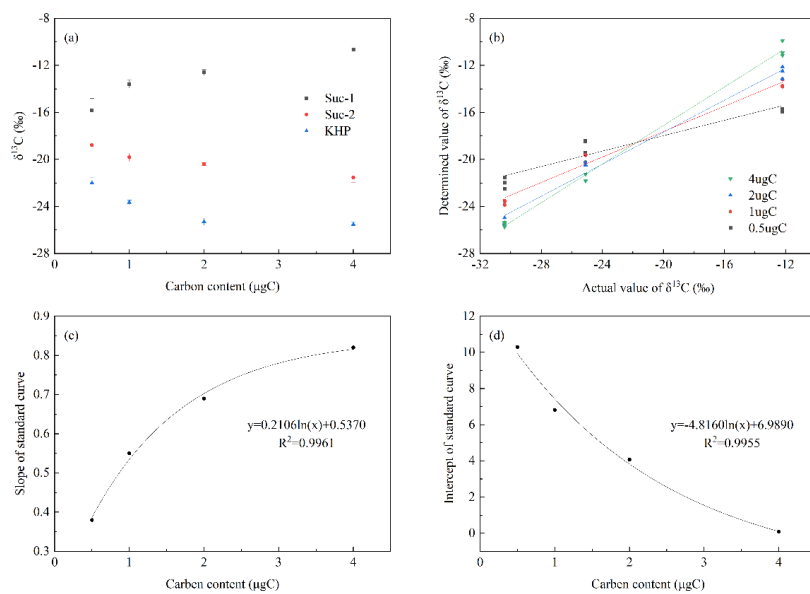
200 Fig 2. Stable carbon isotope ratio determination system

201

202 3. Results and discussion

203 3.1 Improvement of determination method

204 Determination limit was improved to less than $5\mu gC$ in this study (Zhang, et al., 2019).
205 However, determination values have obvious peak area independence in this range of carbon content
206 (Fig. 3a). Based on the consideration of drug solubility in water, three working standards were used
207 in this study in order to establish the standard curve between true value and determination value
208 (Fig. 3b): potassium hydrogen phthalate (KHP) and two kinds of sucrose (Suc-1 and Suc-2) with
209 different $\delta^{13}C$. The carbon isotope composition of these three standards is analyzed by combustion
210 method, using an elemental analyzer combined with an isotope ratio mass spectrometer (EA-IRMS,
211 Thermo Fisher Scientific, USA), as follows: -12.08‰ (Suc-1), -24.83‰ (Suc-2), and -30.62‰
212 (KHP). This range of $\delta^{13}C$ values is able to cover the majority of the $\delta^{13}C$ -WSOC values in ambient
213 air samples. Standards were resolved in Milli-Q water (resistivity $18.2M\Omega$) to make standard
214 solutions of a carbon content of 0.5, 1, 2 and $4\mu g$ in 2mL standard solution to test the procedures
215 during the pretreatment. What's more, it was found in this study that over-heated oxidant would
216 cause severe dilution of $\delta^{13}C$ in standard samples.



217
 218 Fig 3. Determination value of three isotopic working standard with different carbon contents. (a)
 219 Peak area dependent effect of $\delta^{13}\text{C}$; (b) Standard curve with different carbon content; (c) Slope
 220 correction curve of standard curve; (d) Intercept correction curve of standard curve.

221

222 3.2 Component and concentration variation

223 Table 1 Concentration distribution of different components

$\mu\text{g}/\text{m}^3$	WSOC	WSII	$\text{PM}_{2.5}$	Formate	Acetate	Oxalate
Particle phase	15.7 ± 3.9	29.1 ± 13.6	57.0 ± 26.9	0.16 ± 0.07	0.30 ± 0.20	0.18 ± 0.03
Gas phase	42.4 ± 6.0	25.1 ± 10.9		0.54 ± 0.50	5.66 ± 3.23	0.16 ± 0.03

224

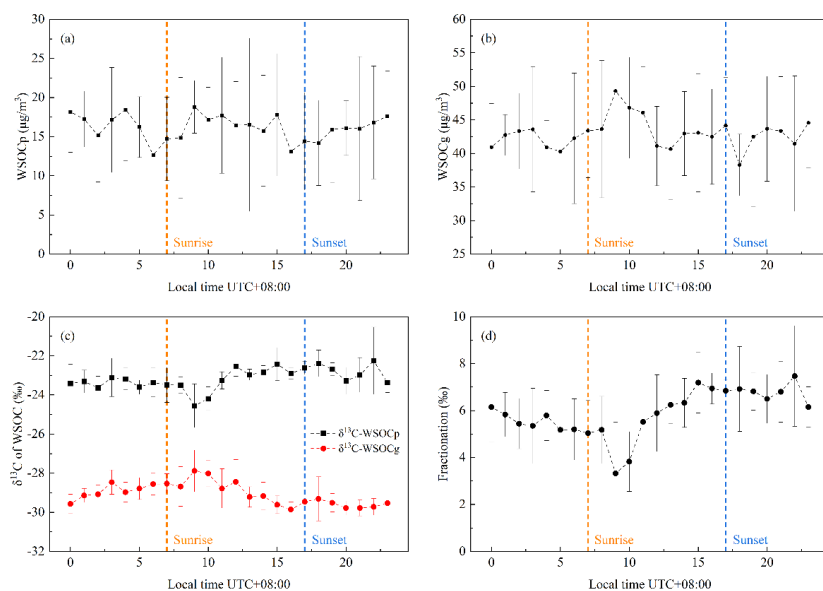
225 During study period, WSOC_p was in the range of 8.7~35.8 $\mu\text{g C m}^{-3}$ and had an average
 226 concentration of $15.7 \pm 3.9 \mu\text{g C m}^{-3}$. WSOC_p accounted for 27.5% of the mass concentration of
 227 $\text{PM}_{2.5}$, and there was a significant correlation between them ($p < 0.01$). The range of WSOC_g
 228 concentrations observed was 25.6~61.2 $\mu\text{g C m}^{-3}$, and the mean concentration was $42.4 \pm 6.0 \mu\text{g C}$
 229 m^{-3} . Overall, there is a very significant level of positive correlation between WSOC_p and WSOC_g
 230 ($p < 0.01$), which indicates a common source of two phases of WSOC. WSOC_p and WSOC_g were
 231 both positively correlated with CO, $\text{PM}_{2.5}$ and PM_{10} ($p < 0.01$), indicating a common CO emission
 232 source of WSOC_p and WSOC_g and the significant contribution of WSOC_g to severe haze



233 pollution. It seems concentration of WSOCg was not affected by meteorological condition in
234 winter, but relative humidity could enhance generation of WSOCp.

235 WSOCp and WSOCg were obvious higher in wintertime. During summertime, WSOCp was
236 in the range of 1.7~12.1 $\mu\text{g C m}^{-3}$ and had an average concentration of $5.9\pm 1.8 \mu\text{g C m}^{-3}$. The
237 range of WSOCg concentrations observed was 16.4~40.0 $\mu\text{g C m}^{-3}$, and the mean concentration
238 was $25.2\pm 5.2 \mu\text{g C m}^{-3}$. Enhancement of WSOCp (166%) was stronger than WSOCg (68%),
239 indicating a more favorable environment for gas phase to particle phase transformation in
240 wintertime.

241 Diurnal profiles of WSOCp and WSOCg were similar, indicating importance of
242 photochemical reaction in WSOC formation (Fig4a, Fig4b). Both WSOCp and WSOCg reached
243 daily maximum concentration at early noon (at 10:00 LT), and reached relatively low
244 concentrations at early morning (about 6:00 LT) and early evening (about 18:00 LT). Differently,
245 there were obvious valley concentration of WSOCp appeared at sunrise and sunset (at 07:00 LT
246 and 17:00 LT), indicating different generation process of WSOCp in daytime and night time.
247 Compared with WSOCp (55%), WSOCg had a relatively lower enhancement (28%) after sunrise.
248 It suggests a substantial regional background and a relatively long lifetime of WSOCg.



249
250 Fig. 4 Diurnal variation distribution (a) Concentration of WSOCp; (b) Concentration of WSOCg;



251 (c) $\delta^{13}\text{C}$ of WSOCp and WSOCg; (d) $\delta^{13}\text{C}$ fractionation between WSOCp and WSOCg.

252

253 Different from similar concentrations of water-soluble inorganic ions (WSII) in two phases,
254 WSOCg was apparently higher than WSOCp, and components of WSOC in different phase may
255 also differed greatly. As a typical component of WSOC, organic acids mainly existed in gas phase.
256 Acetic acid, formic acid and oxalic acid were the main organic acids in WSOC, and the fraction
257 ratios in the particle phase were 0.05, 0.23 and 0.53 respectively.

258

259 3.3 Stable carbon isotopic variation characteristic

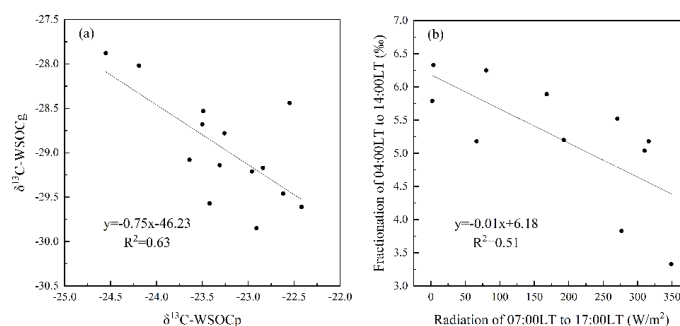
260 WSOCp had a more enriched $\delta^{13}\text{C}$ compared with WSOCg. During study period, $\delta^{13}\text{C}$ -WSOCp
261 was in the range of -22.5~-28.0 ‰ and had an average $\delta^{13}\text{C}$ of -25.9 ± 0.7 ‰, $\delta^{13}\text{C}$ -WSOCg was in
262 the range of -24.3~-31.5 ‰ and had an average $\delta^{13}\text{C}$ of -29.9 ± 0.9 ‰. Both $\delta^{13}\text{C}$ -WSOCp and $\delta^{13}\text{C}$ -
263 WSOCg had an obvious diurnal variation characteristic. $\delta^{13}\text{C}$ -WSOCp was high in night time and
264 low in day time, and $\delta^{13}\text{C}$ -WSOCg was on the contrary. Difference between $\delta^{13}\text{C}$ -WSOCp and $\delta^{13}\text{C}$ -
265 WSOCg reached minimum at around 09:00 LT, and reached maximum at about 23:00 LT (Fig4c).

266 Difference between $\delta^{13}\text{C}$ -WSOCp and $\delta^{13}\text{C}$ -WSOCg, which was considered as isotope
267 fractionation between two phases of WSOC, had negative correlation with concentration of CO 、
268 $\text{PM}_{2.5}$ 、 PM_{10} 、WSOCg and relative humidity (RH) above significant level ($p<0.05$), had positive
269 correlation with O_3 on an extremely significant level in a daily view. However, only O_3 , WSOCg,
270 $\text{PM}_{2.5}$, PM_{10} had extremely significant correlation with $\delta^{13}\text{C}$ -WSOCp, $\delta^{13}\text{C}$ -WSOCg and
271 fractionation at the same time ($p<0.01$). For there was extremely significant positive correlation
272 between fractionation and WSOCg, $\text{PM}_{2.5}$ and PM_{10} , main source of WSOC and its emission
273 intensity may have an obvious diurnal change (Such as liquid fossil-fuel, $\delta^{13}\text{C}$ of which is about -
274 25.5 ± 1.3 ‰(August, et al., 2015)).

275 After distinguishing daytime and nighttime according to radiation intensity, it was found that
276 decrease of temperature and O_3 , along with increase of WSOCg and RH, promoted decreasing of
277 fractionation on an extremely significant level during daytime, and increase of O_3 , $\text{PM}_{2.5}$ and PM_{10}
278 promoted increase of fractionation on an extremely significant level during nighttime ($p<0.01$).
279 Though there was no correlation between fractionation and radiation, there was not only a negative
280 correlation on an extremely significant level ($p<0.01$), but also a highly fitting linear response



281 relationship ($R^2=0.63$) between $\delta^{13}\text{C}\text{-WSOCp}$ and $\delta^{13}\text{C}\text{-WSOCg}$ in an environment with non-zero
282 radiation (Fig5a). It indicated that the mutual conversion between WSOCp and WSOCg may only
283 exists during daytime, and the generations of WSOCp and WSOCg were two independent processes.
284 We also found it was interesting that fractionation had a significant negative correlation with the
285 solar radiation after 3 hours ($p<0.05$), along with a highly fitting linear response relationship
286 ($R^2=0.51$), which was hard to explain (Fig5b).



287
288 Fig. 5 Linear response relationship during daytime (a) $\delta^{13}\text{C}\text{-WSOCp}$ and $\delta^{13}\text{C}\text{-WSOCg}$; (b)
289 Fractionation (04:00LT to 14:00LT) and Radiation (07:00LT to 17:00LT).

290
291 Enrichment of $\delta^{13}\text{C}\text{-WSOCg}$ had an extremely significant correlation with the increase of
292 WSOCp and WSOCg at the same time ($p<0.01$). However, dilution of $\delta^{13}\text{C}\text{-WSOCp}$ only had a
293 significant correlation with the increase of WSOCg ($p<0.05$), with no correlation with WSOCp. It
294 was believed that increase of WSOCp and WSOCg was attributed to changes in emission intensity.
295 WSOCg is more affected by the direct emission source, and WSOCp more from the conversion of
296 gaseous substances rather than direct emission source.

297 3.3 Effects of gaseous pollutants

298 Isotopic fraction of $\delta^{13}\text{C}$ between gas phase and particle phase of WSOCp and WSOCg was
299 considered mainly to mainly come from five parts: isotope fractionation due to gas-particle
300 distribution of SVOC (Vodicka, et al., 2022); isotope fractionation due to equilibrium exchange of
301 WSOCp and WSOCg (Gensch, et al., 2014); isotope changes caused by source proportion changes
302 and emission intensity changes of WSOCp and WSOCg (Saehee, et al., 2020); enrichment of $\delta^{13}\text{C}$
303 caused by retention and aging of WSOCp and WSOCg; isotope fractionation due to proportion



304 change of gas phase reaction and liquid phase reaction in generation process of WSOC_p. According
305 to the principle of isotope mass conservation showed as formula (F1), with a certain mass of SVOC,
306 more gas phase conversion will result in enrichment of $\delta^{13}\text{C}$ -WSOC_p, and more particle phase
307 conversion will result in dilution of $\delta^{13}\text{C}$ -WSOC_g. The conversion of WSOC_p and the dissolution
308 of WSOC_g on the aerosol surface may result in consistent $\delta^{13}\text{C}$ of WSOC_p and WSOC_g due to
309 isotope exchange. Changes in the sources of WSOC_p and WSOC_g will directly cause $\delta^{13}\text{C}$ -WSOC_p
310 and $\delta^{13}\text{C}$ -WSOC_g to approach the $\delta^{13}\text{C}$ of main source(Cao, et al., 2011), and concentration changes
311 of WSOC_p and WSOC_g only happens when emission intensity changes. It had been proved that
312 oxidants in atmosphere tend to react with VOCs which have more depleted $\delta^{13}\text{C}$ (Anderson, et al.,
313 2004; Rudolph, et al., 2003; Rudolph, et al., 2000), leading to a more enriched $\delta^{13}\text{C}$ in residual
314 VOCs. Aged OC in aerosol was also proved to have more enriched $\delta^{13}\text{C}$ (Aggarwal and Kawamura,
315 2008; Pavuluri, et al., 2011; Wang, et al., 2012; Zhang, et al., 2016). Therefore, it's believed that
316 aging of WSOC leads to more enriched $\delta^{13}\text{C}$ -WSOC_p and $\delta^{13}\text{C}$ -WSOC_g. While there is a more
317 enriched $\delta^{13}\text{C}$ in residual VOCs due to reverse kinetic isotope effect of oxidants(Noziere, et al.,
318 2015), SOA generated by gas phase reaction will have more enriched $\delta^{13}\text{C}$, which means $\delta^{13}\text{C}$ of
319 SOA will be depleted when proportion of liquid phase reaction increases. Similarly, it was believed
320 increased proportion of gas phase reaction led to dilution of $\delta^{13}\text{C}$ -WSOC_p, increased proportion
321 of gas phase reaction led to enrichment of $\delta^{13}\text{C}$ -WSOC_p.

$$322 \quad \frac{\text{WSOC}_p \times \delta^{13}\text{C}(\text{WSOC}_p) + \text{WSOC}_g \times \delta^{13}\text{C}(\text{WSOC}_g)}{\text{WSOC}_p + \text{WSOC}_g} = \text{SVOC} \times \delta^{13}\text{C}(\text{SVOC}) \quad (\text{F1})$$

323 In which WSOC_p and WSOC_g are the parts converted from SVOC.

324 Increase of CO led to enrichment of $\delta^{13}\text{C}$ -WSOC_g on an extremely significant level
325 ($p < 0.01$). Though there was also extremely significant positive correlation between concentration
326 of CO and WSOC_p, WSOC_g ($p < 0.01$), along with significant positive correlation between
327 concentration of CO and fp-WSOC ($p < 0.05$), it was difficult for CO to affect conversion between
328 WSOC_p and WSOC_g by participating in the atmospheric chemical reaction. For higher
329 concentration of CO indicated a stronger primary emission source(August, et al., 2015), it was
330 believed that emission of WSOC enhanced in an environment with high concentration of CO,
331 leading generation and retention of plenty of WSOC_g, along with aging of those WSOC_g. However,
332 there was no effect on gas-particle distribution mechanism of WSOC.



333 Increase of NH_3 led to dilution of $\delta^{13}\text{C}$ -WSOCp, enrichment of $\delta^{13}\text{C}$ -WSOCg and increase
334 of WSOCg on an extremely significant level ($p < 0.01$). For there was research found increase of
335 ALWC along with decrease of pH of aerosol in environment of high concentration of NH_3 (Shaojun,
336 et al., 2022), which may be conducive to aerosol release WSOCg. Dilution of WSOCp may come from
337 mutual conversion of WSOCp and WSOCg, while enrichment of $\delta^{13}\text{C}$ -WSOCg may come from aging
338 of WSOCg which was generated in an environment of high concentration of NH_3 considering
339 increasing concentration of WSOCg. There was also possibility of increasing emission intensity of
340 specific source, which led to $\delta^{13}\text{C}$ -WSOCp and $\delta^{13}\text{C}$ -WSOCg tended to be consistent. However,
341 it was hard to explain why there was no significant effect on WSOCp. Considering both $\delta^{13}\text{C}$ -
342 WSOCp and $\delta^{13}\text{C}$ -WSOCg closed to -26% at the same time when fractionation decreased, which
343 is similar to characteristic $\delta^{13}\text{C}$ value of liquid fossil-fuel (August, et al., 2015), it was believed that
344 liquid fossil-fuel was a common source during a period of high concentration of NH_3 .

345 With no correlation with concentration of neither WSOCp nor WSOCg, increase of NO_2 led to
346 dilution of $\delta^{13}\text{C}$ -WSOCp and $\delta^{13}\text{C}$ -WSOCg at the same time on an extremely significant level
347 ($p < 0.01$). For there is dilution of $\delta^{13}\text{C}$ -WSOCp along with enrichment of $\delta^{13}\text{C}$ -WSOCg at the same
348 time, there was little possibility of dilution of $\delta^{13}\text{C}$ -WSOCp caused by mutual conversion of WSOCp
349 and WSOCg. Considering evidence for gas phase reaction of organic nitrates (Alexander, et al., 2019),
350 it was believed that SVOC may be more converted to particle phase, and the gas phase formation
351 reaction of SOA was strengthened under high concentration of NO_2 .

352 Increase of O_3 led to enrichment of $\delta^{13}\text{C}$ -WSOCp and dilution of $\delta^{13}\text{C}$ -WSOCg on an
353 extremely significant level ($p < 0.01$). Similar with NO_2 , neither WSOCp nor WSOCg had correlation
354 with concentration of O_3 , which means none variation of emission intensity of WSOC source when
355 $\delta^{13}\text{C}$ changed. It was believed that SVOC converted more to WSOCp under high concentration of
356 O_3 , leading to dilution of $\delta^{13}\text{C}$ -WSOCg. The aging of WSOCp was promoted at the same time,
357 leading to enrichment of $\delta^{13}\text{C}$ -WSOCp. Dilution of $\delta^{13}\text{C}$ -WSOCg caused by conversion from SVOC
358 to WSOCp exceeded enrichment of $\delta^{13}\text{C}$ -WSOCg caused by aging of WSOCg, leading to a more
359 dilute $\delta^{13}\text{C}$ -WSOCg, indicating that O_3 tends to react with SVOC rather than WSOCg.

360 It seems different gaseous acids had different effects on WSOC. Increase of HONO led to
361 dilution of $\delta^{13}\text{C}$ -WSOCp and enrichment of $\delta^{13}\text{C}$ -WSOCg over a significant level ($p < 0.05$). For
362 there was also extremely significant positive correlation between HONO and WSOCp, WSOCg



363 ($p < 0.01$), emission intensity of WSOC sources may increase under high concentration of HONO,
364 along with mutual conversion of WSOCp and WSOCg. Considering that HONO participates in
365 formation of SOA as an oxidant (Chi, et al., 2022), there was also possibility of enhanced gas phase
366 generation of WSOC led to dilution of $\delta^{13}\text{C}$ -WSOCp. Increase of HCl led to enrichment of
367 $\delta^{13}\text{C}$ -WSOCg and increase of WSOCg on a significant level ($p < 0.05$), with no correlation with $\delta^{13}\text{C}$ -
368 WSOCp. The presence of HCl may inhibit the transformation from WSOCg to WSOCp, promoting
369 the retention and aging of WSOCg. Differs from other acids, gaseous oxalic acid led to dilution
370 of $\delta^{13}\text{C}$ -WSOCg on a significant level ($p < 0.05$) without affecting concentration of WSOCp and
371 WSOCg, which may be caused by the increase in proportion of SVOC conversion to WSOCp.

372 3.4 Effects of component of $\text{PM}_{2.5}$ and gas-particle distribution

373 Increase of $\text{PM}_{2.5}$ and PM_{10} led to enrichment of $\delta^{13}\text{C}$ -WSOCg on an extremely significant
374 level ($p < 0.01$). There was also extremely significant positive correlation between $\text{PM}_{2.5}$, PM_{10} and
375 WSOCp, WSOCg. For there was no correlation between $\text{PM}_{2.5}$, PM_{10} and $\delta^{13}\text{C}$ -WSOCp, it was
376 believed that emission intensity of WSOC sources increased with none change of main source under
377 high concentration of $\text{PM}_{2.5}$ and PM_{10} . Aging of WSOCg and concentration increase of particle
378 matters had consistent atmospheric environmental conditions, and aging of WSOCg may make a
379 considerable contribution to formation of haze.

380 Different components of $\text{PM}_{2.5}$ had different responses to the concentration and isotopes of
381 WSOCp and WSOCg. Consistent with $\text{PM}_{2.5}$ and PM_{10} , SO_4^{2-} , NO_3^- and NH_4^+ (SNA) all had
382 extremely positive correlation with enhancement of $\delta^{13}\text{C}$ -WSOCg, along with increase of WSOCp
383 and WSOCg ($p < 0.01$). Aging of WSOCg may cause generation of haze by participating in formation
384 of SNA. Apart from extremely positive correlation with WSOCp and WSOCg, increase of SO_4^{2-}
385 led to enrichment of $\delta^{13}\text{C}$ -WSOCp on a significant level ($p < 0.05$). For sulfate is largely formed
386 in liquid phases (Gehui, et al., 2018; Gehui, et al., 2016), it was believed that liquid phase generation
387 reaction of WSOCp enhanced during haze period with high concentration of SO_4^{2-} . Increase of NO_2^-
388 led to dilution of $\delta^{13}\text{C}$ -WSOCp on an extremely significant level ($p < 0.01$), indicating a possible
389 enhancement in gas phase generation reaction of WSOCp. However, formation of NO_2^- in
390 atmosphere is still unclear.

391 Generally, $f_p = \text{WSOCp} / (\text{WSOCp} + \text{WSOCg})$ represented gas-particle ratio of WSOC (Hennigan, et
392 al., 2009). f_p of ions was used to represent gas-particle ratio of ions in this research. It was found



393 that though increase of fp of SNA promoted increase of WSOCp and WSOCg in the same time on
394 a significant level ($p < 0.05$), increase of fp-NH₄⁺ only related to enrichment of $\delta^{13}\text{C}$ -WSOCp and
395 increase of fp-NO₃⁻ and fp-SO₄²⁻ only related to enrichment of $\delta^{13}\text{C}$ -WSOCg. Organic nitrate and
396 organic sulfate generated by aged WSOCg may play an important role in gas-particle conversion
397 of nitrate and sulfate. However, it was hard to distinguish contribution by aging of WSOCp, gas
398 conversion of SVOC and liquid phase formation of WSOCp in gas-particle conversion of
399 ammonium, for both of them can lead to enrichment of $\delta^{13}\text{C}$ -WSOCp. Increase of fp-NO₂⁻ led to
400 enrichment of $\delta^{13}\text{C}$ -WSOCp and dilution of $\delta^{13}\text{C}$ -WSOCg on an extremely significant level
401 ($p < 0.01$). Particle conversion of SVOC, liquid phase generation of WSOCp and aging of WSOCp
402 may enhanced in rapid gas-particle conversion of NO₂⁻. However, this was in contradiction with
403 $\delta^{13}\text{C}$ -WSOCp depleted when concentration of NO₂⁻ increased. NO₂⁻ may have other relatively
404 important formation pathways apart from gas-particle conversion from HONO, such as
405 heterogeneous absorption of NO₂ by acetate in WSOCp to generate NO₂⁻ (Wen-Xiu, et al., 2022).
406 Increase of fp-acetate led to increase of WSOCp on an extremely significant level ($p < 0.01$), with
407 none correlation with $\delta^{13}\text{C}$ -WSOC. Acetate may be the main component of WSOCg which
408 converts to particle. Increase of fp-oxalate led to enrichment of $\delta^{13}\text{C}$ -WSOCg on a significant
409 level ($p < 0.05$), with none correlation with concentration of WSOC. Oxalate may be an important
410 component of WSOCg which is easier to aging.

411 3.5 Effects of meteorological conditions

412 Increase of wind speed promoted enrichment of $\delta^{13}\text{C}$ -WSOCp and $\delta^{13}\text{C}$ -WSOCg on an
413 extremely significant level ($p < 0.01$), with no effects on isotope fractionation and concentration of
414 WSOC in two phases. However, change of wind direction could affect fp-WSOC and $\delta^{13}\text{C}$ -WSOCg
415 on an extremely significant level ($p < 0.01$). It was believed that there was a source around sampling
416 site with depleted $\delta^{13}\text{C}$. WSOC transmitted under high wind speed environment mixed with local
417 pollutants, leading to a different source composition. However, gas-particle distribution mechanism
418 of WSOC and emission intensity of pollution sources unchanged. For accidental effects of wind
419 direction was filtered by mean daily analysis, it's believed there existed a strong source of WSOC
420 in the northwest wind direction.

421 Among the other meteorological elements, the increase of temperature promoted enrichment
422 of $\delta^{13}\text{C}$ -WSOCp at a significant level ($p < 0.05$). Increase of atmospheric pressure, RH and radiation



423 intensity promoted the enrichment of $\delta^{13}\text{C}$ -WSOCg above a significant level ($p < 0.05$). The increase
424 of relative humidity, air pressure and radiation may promote the aging of WSOCg. Though
425 conversion of WSOCp to WSOCg can also lead to an enriched $\delta^{13}\text{C}$ -WSOCg, a significant positive
426 correlation between RH and WSOCp ($p < 0.05$) indicated a high possibility that intensity of specific
427 emission source changed in environment with high RH. There was none significant correlation
428 between temperature and concentration of WSOC, indicating that the change of temperature may
429 has no effect on emission intensity. Increase of temperature may be caused enrichment of $\delta^{13}\text{C}$ -
430 WSOCp by promoting more conversion of SVOC to WSOCg and accelerating the aging of WSOCp
431

432 4. Conclusion

433 In this study, we developed a high time resolution method for determining the $\delta^{13}\text{C}$ values of
434 WSOCp and WSOCg by combination of wet oxidation pretreatment and IRMS. With improvement
435 of oxidation method and determination method, $\delta^{13}\text{C}$ value of liquid sample with a carbon content
436 between 0.5 to 5 μg can be determined with an accuracy of 0.6 ‰. Using this method, the $\delta^{13}\text{C}$ value
437 of WSOCp and WSOCg in winter of 2021 at an urban site of Nanjing were determined, which were
438 -25.9 ± 0.7 ‰ and -29.9 ± 0.9 ‰ respectively. Approaching $\delta^{13}\text{C}$ of WSOCp and WSOCg indicted a
439 common source during heavy haze period, which may be liquid fossil fuel.

440 The fractionation between $\delta^{13}\text{C}$ -WSOCp and $\delta^{13}\text{C}$ -WSOCg had a significant diurnal variation
441 of low in the day and high in the night, reaching the lowest at early noon. The existence of sunlight
442 determined whether the formation of WSOCp and WSOCg was an independent chemical process,
443 but there was no correlation between isotope signal and radiation intensity. The fractionation was
444 restricted by WSOCg, RH, O_3 and temperature during daytime, and was restricted by O_3 , $\text{PM}_{2.5}$ and
445 PM_{10} during nighttime. Rise of WSOCg and RH were negative factor for isotope fractionation, and
446 rise of temperature, O_3 , $\text{PM}_{2.5}$ and PM_{10} were positive factor for isotope fractionation.

447 Gas-particle distribution mechanism of WSOC was restricted by meteorological conditions,
448 precursor gaseous pollutants, gaseous oxidants and acid gases, which can lead to isotope dilution
449 and enrichment by affecting gas-particle distribution of SVOC, gas-liquid phase reaction proportion
450 of WSOCp, aging process of WSOCp and WSOCg and gas-particle exchange of WSOC. Gas-
451 particle distribution of SVOC was restricted by NO_2 , O_3 , gaseous oxalic acid and temperature; Gas-
452 liquid phase reaction proportion of WSOCp was restricted by HONO and NO_2 ; Aging process of



453 WSOC_p was restricted by O₃ and temperature; Aging process of WSOC_g was restricted by CO,
454 NH₃, HCl, RH, pressure and radiation; Gas-particle exchange of WSOC was restricted by NH₃, HCl
455 and HONO.

456 In the components of PM_{2.5}, generation of SNA had significant correlation with gas-particle
457 distribution of WSOC. The formation of SNA and WSOC_p was accompanied by the aging of
458 WSOC_g and the enhancement of liquid phase reaction of WSOC_p. Generation of haze may be
459 related to retention and aging of WSOC_g. Reaction between HONO and NO₂⁻ may also have some
460 unknown effects on generation of WSOC through gas phase reaction.

461

462 **Author Contribution**

463 Hao-Ran Yu and Yan-Lin Zhang designed the experiments; Hao-Ran Yu adapted the instruments,
464 carried out isotope test; Fang Cao, Xiao-Ying Yang, Tian Xie and Yu-Xian Zhang organized the
465 sampling, Yongwen Xue carried out TOC test. Hao-Ran Yu prepared the manuscript with
466 contributions from all co-authors.

467

468 **Competing Interests**

469 The authors declare that they have no conflict of interest.

470

471 **Acknowledgements**

472 This work was supported by the National Natural Science Foundation of China (No. 41977305)
473 and Jiangsu Innovation & Entrepreneurship Team. The authors declare no competing financial
474 interest.

475

476 **Reference**

477 Aggarwal S. G., Kawamura K.: Molecular distributions and stable carbon isotopic compositions of
478 dicarboxylic acids and related compounds in aerosols from Sapporo, Japan: Implications for
479 photochemical aging during long-range atmospheric transport, *Journal of Geophysical Research*, 113:
480 D14301, 10.1029/2007jd009365, 2008.
481 Alexander Becky, Sherwen Tomas, Holmes Christopher, Fisher A. Jenny, Chen Qianjie, Evans Mat,
482 Kasibhatla Prasad: Global Inorganic Nitrate Production Mechanisms: Comparison of a Global Model



- 483 with Nitrate Isotope Observations, *Atmospheric Chemistry and Physics*, 20: 3859–3877, 2019.
- 484 Anderson Casey H., Dibb Jack E., Griffin Robert J., Hagler Gayle S. W., Bergin Michael H.: Atmospheric
485 water-soluble organic carbon measurements at Summit, Greenland, *Atmospheric Environment*, 42(22):
486 5612-5621, 10.1016/j.atmosenv.2008.03.006, 2008.
- 487 Anderson R. S., Iannone R., Thompson A. E., Rudolph J., Huang L.: Carbon kinetic isotope effects in
488 the gas-phase reactions of aromatic hydrocarbons with the OH radical at 296 +/- 4 K, , *Geophysical
489 Research Letters*, 31: 15108, 10.1029/2004gl020089, 2004.
- 490 August Andersson, Junjun Deng, Ke Du, Mei Zheng, Caiqing Yan, Martin SköLd, Örjan Gustafsson:
491 Regionally-Varying Combustion Sources of the January 2013 Severe Haze Events over Eastern China,
492 *Environment Science & Technology*, 49: 2038-2043, 10.1021/es503855e, 2015.
- 493 Bond T. C., Doherty S. J., Fahey D. W., Forster P. M., Berntsen T., Deangelo B. J., Flanner M. G., Ghan
494 S., Karcher B., Koch D., Kinne S., Kondo Y., Quinn P. K., Sarofim M. C., Schultz M. G., Schulz M.,
495 Venkataraman C., Zhang H., Zhang S., Bellouin N., Guttikunda S. K., Hopke P. K., Jacobson M. Z.,
496 Kaiser J. W., Klimont Z., Lohmann U., Schwarz J. P., Shindell D., Storelvmo T., Warren S. G., Zender
497 C. S.: Bounding the role of black carbon in the climate system: A scientific assessment, *Journal of
498 Geophysical Research*, 118: 5380-5552, 10.1002/jgrd.50171, 2013.
- 499 Cao J. J., Chow J. C., Tao J., Lee S. C., Watson J. G., Ho K. F., Wang G. H., Zhu C. S., Han Y. M. : Stable
500 carbon isotopes in aerosols from Chinese cities: Influence of fossil fuels *Atmospheric Environment*, 45:
501 1359-1363, 10.1016/j.atmosenv.2010.10.056, 2011.
- 502 Carlton A. G., Turpin B. J. : Particle partitioning potential of organic compounds is highest in the Eastern
503 US and driven by anthropogenic water, *Atmospheric Chemistry and Physics*, 13: 10203-10214,
504 10.5194/acp-13-10203-2013, 2013.
- 505 Carlton A. G., Wiedinmyer C., Kroll J. H.: A review of Secondary Organic Aerosol (SOA) formation
506 from isoprene, *Atmospheric Chemistry and Physics*, 9: 4987-5005, 10.5194/acp-9-4987-2009, 2009.
- 507 Chi Yang, Shuxin Zhou, Chunyan Zhang, Mingyuan Yu, Fang Cao, Yanlin Zhang: Atmospheric
508 Chemistry of Oxalate: Insight Into the Role of Relative Humidity and AerosolAcidity From High-
509 Resolution Observation, *Journal of Geophysical Research: Atmospheres*, 127(4): e2021JD035364,
510 10.1029/2021jd035364, 2022.
- 511 El-Sayed Marwa M. H., Wang Yingqing, Hennigan Christopher J.: Direct atmospheric evidence for the
512 irreversible formation of aqueous secondary organic aerosol, *Geophysical Research Letters*, 42(13):
513 5577-5586, 10.1002/2015gl064556, 2015.
- 514 Fisseha R., Saurer M., Jaggi M., Szidat S., Siegwolf R. T., Baltensperger U.: Determination of stable
515 carbon isotopes of organic acids and carbonaceous
516 aerosols in the atmosphere, *Rapid Commun Mass Spectrom*, 20(15): 2343 - 2347, 10.1002/rcm.2586,
517 2006.
- 518 Fu P., Kawamura K., Usukura K., Miura K.: Dicarboxylic acids, ketocarboxylic acids and glyoxal in the
519 marine aerosols collected during a round-the-world cruise, *Marine Chemistry*, 148: 22-32,
520 10.1016/j.marchem.2012.11.002, 2013.
- 521 Gehui Wang, Fang Zhang, Jianfei Peng, Lian Duan, Yuemeng Ji, Wilmarie Marrero-Ortiz, Jiayuan Wang,
522 Jianjun Li, Can Wu, Cong Cao, Yuan Wang, Jun Zheng , Jeremiah Secrest, Yixin Li, Yuying Wang, Hong
523 Li, Na Li, Renyi Zhang: Particle acidity and sulfate production during severe haze events in China cannot
524 be reliably inferred by assuming a mixture of inorganic salts, *Atmospheric Chemistry and Physic*, 18:
525 10123-10132, 10.5194/acp-18-10123-2018, 2018.
- 526 Gehui Wang, Renyi Zhang, Mario E. Gomez, Lingxiao Yang, Misti Levy Zamora, Min Hu, Yun Lin,



- 527 Jianfei Peng, Song Guo, Jingjing Meng, Jianjun Lia, Chunlei Cheng, Tafeng Hu, Yanqin Ren, Yuesi Wang,
528 Jian Gao, Junji Cao, Zhisheng An, Weijian Zhou, Guohui Lia, Jiayuan Wang, Pengfei Tian, Wilmarie
529 Marrero-Ortiz, Jeremiah Secrest, Zhuofei Du, Jing Zheng, Dongjie Shang, Limin Zeng, Min Shao,
530 Weigang Wang, Yao Huang, Yuan Wang, Yujiao Zhu, Yixin Li, Jiayi Hu, Bowen Pan, Li Cai, Yuting
531 Cheng, Yuemeng Ji, Fang Zhang, Daniel Rosenfeld, Peter S. Liss, Robert A. Duce, Charles E. Kolb,
532 Mario J. Molina: Persistent sulfate formation from London Fog to Chinese haze, *Proceedings of the*
533 *National Academy of Sciences of the United States of America*, 113(48): 13630–13635,
534 10.1073/pnas.1616540113, 2016.
- 535 Gensch I., Kiendler-Scharr A., Rudolph J., . . . 206–221. <https://doi.org/>: Isotope ratio studies of
536 atmospheric organic compounds: principles, methods, applications and potential, *International Journal*
537 *of Mass Spectrometry*, 365–366: 206–221, 10.1016/j.ijms.2014.02.004., 2014.
- 538 Hennigan C. J., Bergin M. H., Russell A. G., Nenes A., Weber R. J.: Gas/particle partitioning of water-
539 soluble organic aerosol in Atlanta, *Atmospheric Chemistry and Physics*, 9: 3613–3628, 10.5194/acp-9-
540 3613-2009, 2009.
- 541 Ho K. F., Cao J. J., Lee S. C., Kawamura K., Zhang R. J., Chow J. C., Watson J. G.: Dicarboxylic acids,
542 ketocarboxylic acids and dicarbonyls in urban atmosphere of China., *Journal of Geophysical Research*,
543 112: D22S27, 10.1029/2006JD008011, 2006.
- 544 Jingyue Tang, Liming Zeng, Huabin Dong: A new method for on-line measurements of water-soluble
545 organic compounds, *Acta Scientiae Circumstantiae*, 30(5): 908-914, 10.1631/jzus.A1000244, 2010.
- 546 Kondo Y., Miyazaki Y., Takegawa N., Miyakawa T., Weber R. J., Jimenez J. L., Zhang Q., Worsnop D.
547 R.: Oxygenated and water-soluble organic aerosols in Tokyo, *Journal of Geophysical Research*, 112:
548 D01203, 10.1029/2006jd007056, 2007.
- 549 Lewtas Joellen, Pang Yanbo, Booth Derrick, Reimer Steve, Eatough Delbert J., Gundel Lara A.:
550 Comparison of Sampling Methods for Semi-Volatile Organic Carbon Associated with PM_{2.5}, *Aerosol*
551 *Science and Technology*, 34(1): 9-22, 10.1080/02786820118935, 2001.
- 552 Liu J. M., Zhang X. L., Parker E. T., Veres P. R., Roberts J. M., De Gouw J. A., Hayes P. L., Jimenez J.
553 L., Murphy J. G., Ellis R. A., Huey L. G., Weber R. J.: On the gas-particle partitioning of soluble organic
554 aerosol in two urban atmospheres with contrasting emissions: 2. Gas and particle phase formic acid,
555 *Journal of Geophysical Research: Atmospheres*, 117(D21): D00V21, 10.1029/2012JD017912, 2012.
- 556 Liu S., Ahlm L., Day D. A., Russell L. M., Zhao Y. L., Gentner D. R., Weber R. J., Goldstein A. H., Jaoui
557 M., Offenberg J. H., Kleindienst T. E., Rubitschun C., Surratt J. D., Sheesley R. J., Scheller S.: Secondary
558 organic aerosol formation from fossil fuel sources contribute majority of summertime organic mass at
559 Bakersfield, *Journal of Geophysical Research: Atmospheres*, 117(D24): D00V26,
560 10.1029/2012JD018170, 2012.
- 561 Lv S., Wang F., Wu C., Chen Y., Liu S., Zhang S., Li D., Du W., Zhang F., Wang H., Huang C., Fu Q.,
562 Duan Y., Wang G.: Gas-to-Aerosol Phase Partitioning of Atmospheric Water-Soluble Organic
563 Compounds at a Rural Site in China: An Enhancing Effect of NH₃ on SOA Formation, *Environmental*
564 *Science & Technology*, 56(7): 3915-3924, 10.1021/acs.est.1c06855, 2022.
- 565 Meng J. J., Wang G. H., Li J. J., Cheng C. L., Ren Y. Q., Huang Y., Cheng Y. T., Cao J. J., Zhang T.:
566 Seasonal characteristics of oxalic acid and related SOA in the free troposphere of Mt. Hua, central China:
567 Implications for sources and formation mechanisms, *Science of Total Environment*, 493: 1088-1097,
568 10.1016/j.scitotenv.2014.04.086, 2014.
- 569 Miyazaki Y., Kondo Y., Takegawa N., Komazaki Y., Fukuda M., Kawamura K., Mochida M., Okuzawa
570 K., Weber R. J.: Time-resolved measurements of water-soluble organic carbon in Tokyo, *Journal of*



- 571 Geophysical Research, 111: D23206, 10.1029/2006JD007125, 2006.
- 572 Noziere B., Kalberer M., Claeys M., Allan J., D'anna B., Decesari S., Finessi E., Glasius M., Grgic I.,
573 Hamilton J. F., Hoffmann T., Iinuma Y., Jaoui M., Kahnt A., Kampf C. J., Kourtchev I., Maenhaut W.,
574 Marsden N., Saarikoski S., Schnelle-Kreis J., Surratt J. D., Szidat S., Szmigielski R., Wisthaler A.: The
575 molecular identification of organic compounds in the atmosphere: state of the art and challenges,
576 Chemical Reviews, 115: 3919-3983, 10.1021/cr5003485, 2015.
- 577 Pavuluri C. M., Kawamura K., Swaminathan T., Tachibana E.: Stable carbon isotopic compositions of
578 total carbon, dicarboxylic acids and glyoxylic acid in the tropical Indian aerosols: Implications for
579 sources and photochemical processing of organic aerosols, Journal of Geophysical Research, 116:
580 D18307, 10.1029/2011jd015617, 2011.
- 581 Pöschl U.: Atmospheric aerosols: composition, transformation, climate and health effects, Angewandte
582 Chemie-International Edition, 44: 7520-7540, 10.1002/anie.200501122, 2005.
- 583 Rudolph J., Anderson R. S., Czapiewski K. V., Czuba E., Ernst D., Gillespie T., Huang L., Rigby C.,
584 Thompson A. E.: The stable carbon isotope ratio of biogenic emissions of isoprene and the potential use
585 of stable isotope ratio measurements to study photochemical processing of isoprene in the atmosphere,
586 Journal of Atmospheric Chemistry, 44,: 39-55, 10.1023/A:1022116304550, 2003.
- 587 Rudolph J., Czuba E., Huang L.: The stable carbon isotope fractionation for reactions of selected
588 hydrocarbons with OH-radicals and its relevance for atmospheric chemistry, Journal of Geophysical
589 Research, 105(D24): 29329-29346, 10.1029/2000JD900447, 2000.
- 590 Saehee Lim, Xiaoyang Yang, Meehye Lee, Gang Li, Yuanguan Gao, Xiaona Shang, Kai Zhang, Claudia
591 I. Czimeczik, Xiaomei Xu, Min-Suk Bae, Kwang-Joo Moon, Kwonho Jeon: Fossil-driven secondary
592 inorganic PM_{2.5} enhancement in the North China Plain: Evidence from carbon and nitrogen isotopes,
593 Environmental Pollution, 266: 115163, 10.1016/j.envpol.2020.115163, 2020.
- 594 Sareen N., Waxman E. M., Turpin B. J., Volkamer R., Carlton A. G.: Potential of Aerosol Liquid Water
595 to Facilitate Organic Aerosol Formation: Assessing Knowledge Gaps about Precursors and Partitioning,
596 Environmental Science & Technology, 51: 3327-3335, 10.1021/acs.est.6b04540, 2017.
- 597 Shaojun Lv, Fanglin Wang, Can Wu, Yubao Chen, Shijie Liu, Si Zhang, Dapeng Li, Wei Du, Fan Zhang,
598 Hongli Wang, Cheng Huang, Qingyan Fu, Yusen Duan, Gehui Wang: Gas-to-Aerosol Phase Partitioning
599 of Atmospheric Water-Soluble Organic Compounds at a Rural Site in China: An Enhancing Effect of
600 NH₃ on SOA Formation, Environmental Science & Technology, 56(7): 3915-3924,
601 10.1021/acs.est.1c06855, 2022.
- 602 Suto N., Kawashima H.: Online wet oxidation/isotope ratio mass spectrometry method for determination
603 of stable carbon isotope ratios of water-soluble organic carbon in particulate matter, Rapid Commun
604 Mass Spectrom, 32(19): 1668-1674, 10.1002/rcm.8240, 2018.
- 605 Vodicka P., Kawamura K., Schwarz J., Zdimar V.: Seasonal changes in stable carbon isotopic composition
606 in the bulk aerosol and gas phases at a suburban site in Prague, Science of Total Environment, 803:
607 149767, 10.1016/j.scitotenv.2021.149767, 2022.
- 608 Wang G. H., Kawamura K., Cheng C. L., Li J. J., Cao J. J., Zhang R. J., Zhang T., Liu S. X., Zhao Z. Z.:
609 Molecular Distribution and Stable Carbon Isotopic Composition of Dicarboxylic Acids, Ketocarboxylic
610 Acids, and alpha-Dicarbonyls in Size-Resolved Atmospheric Particles From Xi'an City, China,
611 Environmental Science & Technology, 46: 4783-4791, 10.1021/es204322c, 2012.
- 612 Weber R. J., Sullivan A. P., Peltier R. E., Russell A., Yan B., Zheng M., Gouw J., Warneke C., Brock C.,
613 Holloway J. S., Atlas E. L., Edgerton E.: A study of secondary organic aerosol formation in the
614 anthropogenic-influenced southeastern United States, Journal of Geophysical Research, 112: D13302,



615 10.1029/2007JD008408, 2007.
616 Wen-Xiu Pei, Shuai-Shuai Ma, Zhe Chen, Yue Zhu, Shu-Feng Pang, Yun-Hong Zhang: Heterogeneous
617 uptake of NO₂ by sodium acetate droplets and secondary nitrite aerosol formation, *Journal of*
618 *Environmental Sciences*, : 10.1016/j.jes.2022.05.04, 2022.
619 Yang Li, Shang Yue, Hannigan Michael P., Zhu Rui, Wang Qin'geng, Qin Chao, Xie Mingjie: Collocated
620 speciation of PM_{2.5} using tandem quartz filters in northern nanjing, China: Sampling artifacts and
621 measurement uncertainty, *Atmospheric Environment*, 246: 10.1016/j.atmosenv.2020.118066, 2021.
622 Zhang Wenqi, Zhang Yan-Lin, Cao Fang, Xiang Yankun, Zhang Yuanyuan, Bao Mengying, Liu Xiaoyan,
623 Lin Yu-Chi: High time-resolved measurement of stable carbon isotope composition in water-soluble
624 organic aerosols: method optimization and a case study during winter haze in eastern China, *Atmospheric*
625 *Chemistry and Physics*, 19(17): 11071-11087, 10.5194/acp-19-11071-2019, 2019.
626 Zhang X. L., Liu J. M., Parker E. T., Hayes P. L., Jimenez J. L., De Gouw J. A., Flynn J. H., Grossberg
627 N., Lefer B. L., Weber R. J.: On the gas-particle partitioning of soluble organic aerosol in two urban
628 atmospheres with contrasting emissions: 1. Bulk water-soluble organic carbon, *Journal of Geophysical*
629 *Research: Atmospheres*, 117(D21): D00V21, 10.1016/j.atmosenv.2013.04.060, 2012.
630 Zhang Y. L., Kawamura K., Cao F., Lee M.: Stable carbon isotopic compositions of low - molecular -
631 weight dicarboxylic acids, oxocarboxylic acids, α - dicarbonyls, and fatty acids: Implications for
632 atmospheric processing of organic aerosols, *Journal of Geophysical Research*, 121: 3707-3717,
633 10.1002/2015jd024081, 2016.
634